Micro-Jet Ventilation – a Novel Ventilation Concept for long-range Aircraft Cabins

Tobias Dehne, MEng
Non-Member ASHRAE

Pascal Lange, MEng
Non-Member ASHRAE

Dr. Daniel Schmeling
Non-Member ASHRAE

Dipl. Ing. Ingo Gores
Non-Member ASHRAE

ABSTRACT

Micro-Jet Ventilation (MJV), known from ventilation systems in trains, was experimentally investigated under static flight conditions in a full-scale twin-aisle cabin mock-up as part of the Clean-Sky 2 Joint Undertaking project ADVENT. A jacket cooling system was used to investigate ventilation systems for aircraft cabins with thermodynamically realistic boundary conditions. Temperature-controlled thermal manikins (TMs) make it possible to simulate the heat dissipation and obstruction of real passengers. In this study, six different modifications of MJV with different air inlet configurations are analyzed to determine the optimal parameters for thermal comfort and energy savings. Fluid temperatures as well as velocities in the vicinity of the TMs were investigated using high-resolution local probes. An evaluation of the various MJV configurations was performed based on heat removal efficiency, thermal comfort parameters, and tracer gas analysis. The study clearly shows the near-optimal comfort parameters of two MJV configurations for future aircraft cabins.

INTRODUCTION

Novel ventilation systems for aircraft cabins have attracted the attention of scientists and aircraft manufacturers during the last years due to their potential of energy saving as well as a higher level of thermal comfort. Technical innovations at all levels of aircraft design are needed to reduce CO2 emissions from the global fleet by 50% by 2050, for more information see IATA (2009). Furthermore, the Environmental Control System (ECS) needs up to 75% of non-propulsive power for conditioning of a passenger aircraft under normal flight conditions cruise as shown in Martinez (2014). With a general trend of rising heat loads in modern passenger cabins, the interest of the aircraft industry in novel ventilation systems is of high importance. Further challenges are an improved thermal passenger comfort, a higher air quality level as well as the opportunity to reconsider the cabin layout. Therefore, previous studies deal with numerical as well as experimental investigations of alternative ventilation systems in single as well as twin aisle aircraft cabins. One example is cabin displacement ventilation (CDV) (Yin et al. 2007, Schmidt 2008, Zhang et al. 2009), in which fresh air is supplied at low momentum. Among other things, this results in high heat removal and low draft rates; for more details, see Bosbach et al. (2013). To evaluate novel ventilation concepts under realistic stationary as well as non-stationary boundary conditions, flight tests were conducted in an A320 of the German Aerospace

Tobias Dehne and **Pascal Lange** are technical employees**, Daniel Schmeling** is a research associate and team leader at the Institute of Aerodynamics and Flow Technology of the German Aerospace Center (DLR), Goettingen, Germany. **Ingo Gores** is a ventilation expert at Airbus Germany GmbH

Center (DLR) and analysed in Bosbach et al. (2012). During these pioneering, but also very expensive, measurement flights different thermodynamic boundary conditions depending on the flight and operational phases were recorded in Dehne et al. (2014). To avoid high costs with time exposure for further flight tests and allow for a greener and smarter testing of novel ventilation concepts for future long-range airliners, a full-scale twin aisle cabin mock-up with thermodynamically realistic boundary conditions by means of temperature-controlled fuselage elements was developed at the DLR in Göttingen, for details visit Lange et al. (2020). The modular construction of the new facility allows the installation of different cabin geometries while simultaneously providing a high flexibility for the integration of novel ventilation concepts. Further, different flight phases with operationally relevant temperature and time scales can be simulated. In Lange et al. (2021), MJV, which is known as a ventilation system in trains (Schmeling et al. 2020-2), was analyzed for two different operational scenarios: the normal "cruise" flight condition and the "hot-day-on-ground" scenario, which represents the departure of an aircraft in very warm ambient temperatures. A volume flow rate of 50 % to 50 % between straight and slanted outlets was investigated.

The aim of the present study is a deeper evaluation of MJV in the new full-scale, long-range aircraft cabin mock-up. In order to determine optimal comfort parameters for the passengers, six different volume flow distributions were experimentally investigated under the realistic flight phase Cruise with cold ambient conditions. 100 thermal manikins were used to simulate the obstructions and the heat release of real passengers. Several measurement techniques were used in order to quantify and evaluate the following parameters: boundary conditions, cabin air temperature, ventilation efficiency, thermal comfort, fluid velocities and particle distribution. The present work is of great importance in order to determine the optimal volume flow distribution for future comparisons with the reference case of state-of-the-art mixing ventilation (MV) as well as other novel ventilation systems.

1 TEST ENVIRONMENT AND VENTILATION SYSTEM

MJV was investigated with different modifications in the full-scale twin aisle mock-up. MJV, which is state-of-the-art for air-conditioning of trains, is characterized by a high degree of mixing by jets of fresh air entering the cabin in the aisle area (Schmeling, 2020-2). A perforated ceiling brings the air into the passenger compartment as localized micro jets with high momentum.

Table 1. Investigated test cases with boundary conditions for Micro-Jet Ventilation

Case	Ambient Conditions	Volume Flow (V) [m³/s]	V Slanted [m³/s]	V Straight [m³/s]	T_{cab} [°C] / [°F]	T_{amb} [°C] / [°F]	T_{in} [°C] / [°F]	T_{out} [°C] / [°F]
100/ - 0|	Cruise	1	1	0	23.0 / 73.4	10.2 / 50.4	19.6 / 67.3	21.5 / 70.7
66/ - 33|			0.67	0.67	23.0 / 73.4	10.0 / 50.0	18.8 / 65.8	20.3 / 68.5
50/ - 50|			0.5	0.5	22.9 / 73.2	10.5 / 50.9	18.0 / 64.4	20.8 / 69.4
33/ - 66|			0.33	0.33	23.1 / 73.6	9.9 / 49.8	18.8 / 65.8	20.5 / 68.9
0/ - 100|			0	1	23.0 / 73.4	10.2 / 50.4	18.6 / 65.5	19.3 / 66.7
MIX			See Figure 1b)		23.1 / 73.4	10.6 / 51.0	19.3 / 66.7	20.7 / 69.3

The entire area above the aisle is equipped with two slanted as well as two straight micro-jet air inlets in cross-section, see Figure 1 (left). With nine inlets in longitudinal direction, overall 36 air inlets were installed in the mock-up (Figure 1 (right)). The exhaust air openings are located in the lower part on both sides of the cabin (red arrows, Figure 1 (left)) close to the Dado panels. For more details, also on the air ducts out of the cabin mock-up, see Lange et al. (2020). To determine the optimal thermal comfort and energy efficiency settings, the volume flow was split to six different distributions in terms of slanted and straight MJV inlets under cruise conditions. All investigated cases with boundary conditions are summarized in Table 1, named after the percentage distribution of slanted (/) and horizontal (|) air inlet supply. The “MIX” case is a distribution of 66% - 33% volume flow like the checkerboard in Figure 1 (right). To investigate the MJV cases under real flight conditions, a jacket heating/cooling based on capillary tubes was implemented in the structure of the cabin mock-up, see Lange et al. (2020). In this study, we concentrate on the normal flight level “cruise” with gap (between primary and secondary insulation) temperatures of 10 °C / 50 °F. For

all cases, the incoming air temperature was adjusted to reach a cabin air temperature of 23 °C / 73.4 °F. Table 1 shows the averaged values for supply air T_{in}, exhaust air T_{out}, the mean cabin temperature T_{cab} as well as for the ambient temperatures T_{amb}. Deviations of T_{cab} as small as 0.1 K (Table 1) were achieved, reflecting the high precision of the temperature control system in the new mock-up.

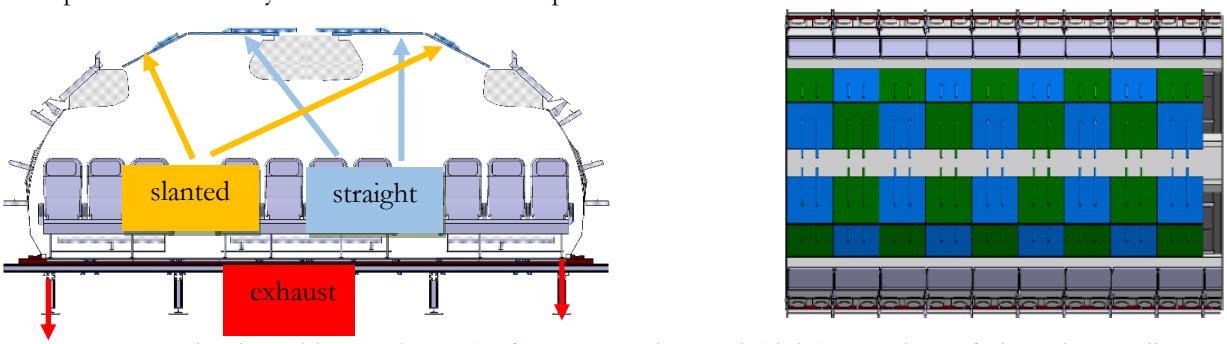

Figure 1: MJV in the cabin mock-up. (Left) cross-section and (right) top view of slanted as well as straight mounted air inlets. Additionally, (right) shows the checkerboard of "MIX" combination between slanted and straight air inlets. Here, the volume flow was split as follows: 66% air inlets in green and 33% air inlets in blue.

2 EXPERIMENTAL SETUP

With the aim to investigate novel ventilation concepts in a realistic measurement environment, a full-scale cabin mock-up was developed and constructed at the German Aerospace Center (DLR) in Göttingen (Lange et al. 2020).

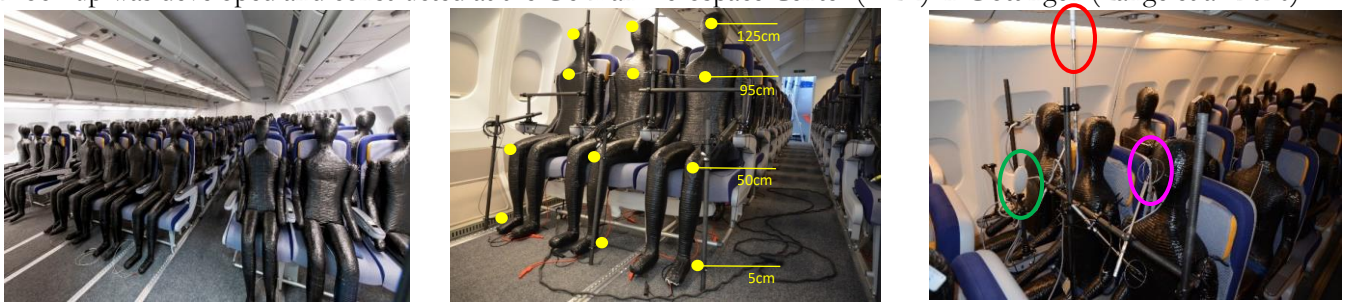

a) **b)** **c)**

Figure 2: a) Interior of cabin mock-up with TMs, b) measurement racks with resistance temperature detectors (RTDs) on four height and c) measurement racks with omnidirectional velocity sensors (magenta circle) as well as humidity (red circle) and operative temperature probe (green circle) in the vicinity of the TMs in row 6.

To ensure realistic heat loads and obstruction, which are important for the generation of buoyancy forces and dissipation of momentum, TMs were used for the experimental studies, see Figure 2 a). The thermal manikins consist of a foam core wrapped with a resistance wire and a thin layer of black heat-conductive aluminum. Each TM, with a volume of 0.05 m^3 and a surface of 1.52 m^2, can be heated individually by an external power supply to provide a constant sensible heat release in a range of 0 to 150 W. For this study, the TMs operated with an automatic control of the heat release depending on the mean temperature in the cabin which provides a realistic simulation of the human metabolism. The underlying human heat release – cabin temperature curve – is based on a standard (EN13129) and represents a value of 82 W for a T_{cab} of 23 °C / 73.4 °F.

To evaluate temperature stratification near the TMs as well as in a complete row of seats, ten measuring stations with resistance temperature detectors (RTDs) were installed at four height levels near the TMs at a distance of 5 cm, exemplified in Figure 2 b). One additional rack with RTDs at 12 different heights was positioned in the left aisle section in row 5 to evaluate temperature stratification in the aisle. RTDs at chest height were installed in front of all TMs for the acquisition of the temperature homogeneity in the complete cabin, for details see Lange (2021).

The flow velocities in the cabin, measured with a distance of 5 cm to the TMs at four height levels on 10 seats in

row 6 (Figure 2 c), are important for two reasons: First, the velocity should be low enough to prevent draft. Second, the large-scale flow patterns and small-scale turbulence structures of the cabin flow determine the mixing and heat exchange and thus macroscopic quantities such as heat dissipation, temperature homogeneity and temperature stratification. Additionally, the probes in row 6 are able to measure the fluid temperatures. They provide an accuracy of 0.02 m/s for the velocity and 0.2 K for the temperature. Using these probes, the comfort-relevant air velocities and their distribution for different body parts and seat rows were captured. The system is combined with a humidity as well as an operative temperature probe to determine the Predicted Mean Vote (PMV) and Predicted Percentage Dissatisfied (PPD), see Figure 2 c).

The propagation of containments such as pathogenic organisms plays a significant role in aircraft with a high passenger density. By means of a multi-gas monitoring system, the propagation of particles was investigated using Sulphur hexafluoride (SF6) as tracer gas. For the dispersion analysis, the distribution in cross (1 seat left / right next to the source) as well as longitudinal (2 seats in front / back to the source) direction was recorded at 6 seat positions originating from seat 8H. Nylon tubes with an internal diameter of 3 mm and a length of 50 m provide an accuracy of dosage calculation of ± 2%.

3 RESULTS

3.1 Temperatures. In this chapter, the temperatures for all investigated flow distributions under MJV conditions are discussed. Figure 3 shows the mean temperatures in the vicinity of the TMs averaged over 1800 s at four height levels (ankle, knee, chest, head) in row 4. Further, the standard deviations for all temperatures are discussed.

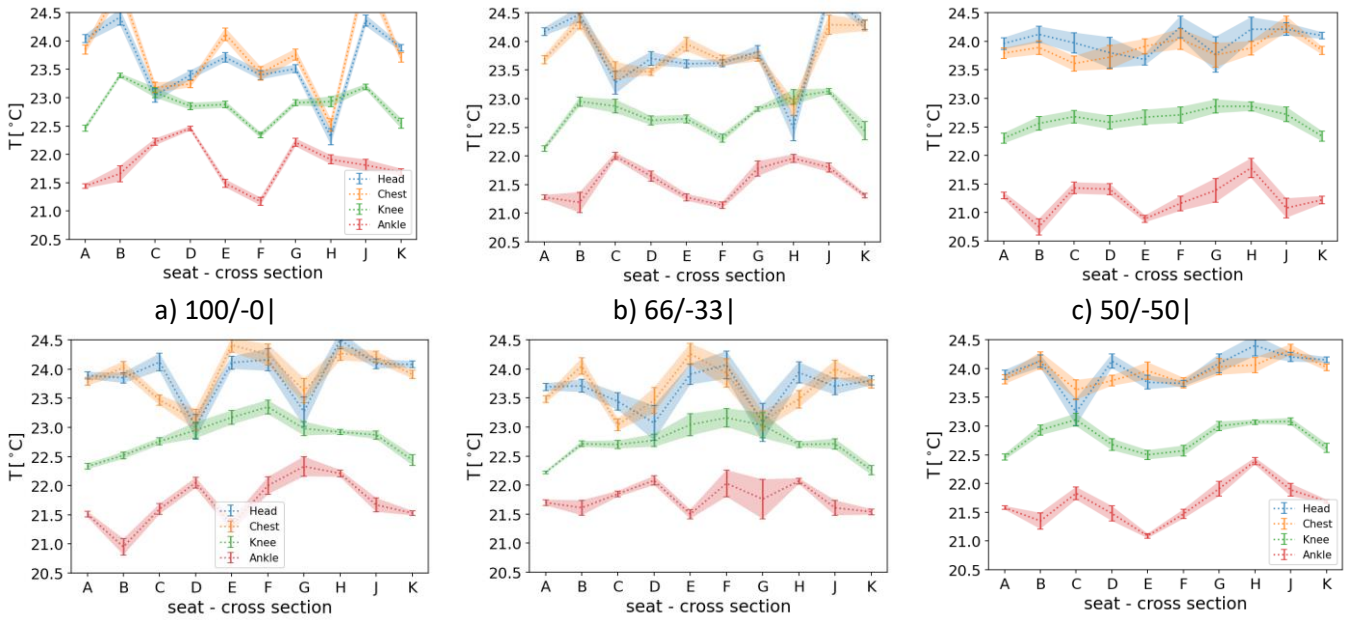

Figure 3: Comparison of fluid temperatures in the vicinity of the TMs at four height positions for a) 100/-0|, b) 66/-33|, c) 50/-50|, d) 33/-66|, e) 0/-100| and f) MIX

First it should be noted that all temperature distributions are homogeneous conditions with a temperature range of ±1 K for all cases except 100/-0| and 66/-33| reflect. A higher proportion of slanted air supply reflects in higher temperature differences, particularly in flight direction left (FDL) for seat B and C as well as right (FDR) for seat H and J. When discussing this high level of homogeneity, the best results can be observed for 50/-50| and MIX with fluctuations of 0.31 K and 0.23 K, respectively. The maximum standard deviation of 0.34 K (0/-100|) shows a good homogeneity of the ventilation system due to temperatures on different height levels near the TMs.

For the evaluation of the investigated MJV variants, the maximum (ΔTh-amax) and mean (ΔTh-amean) temperature differences between head and ankle as well as between maximum and minimum chest temperatures differences (ΔTchest) are pivotal. They are pointed out in Table 2 with temperature deviations less than 2.0 K marked in green, larger than 4.0 in red and intermediate values in yellow after ASHRAE (2001). Here the maximum temperature stratification (ΔTh-amax) is up to 3.4 K near the TMs for 66/-33| and 50/-50|. The mean temperature stratifications ($\Delta T_{h\text{-}a}^{mean}$) reveal acceptable results for all concepts, with the lowest temperature differences <2 K for the cases 100/-0| and 0/-100|. Regarding the chest temperature differences, all ventilation concepts were evaluated as acceptable, too. However, a higher proportion of straight air supply reflects in lower temperature differences.

The mean temperatures per row (averaged on chest level), reveal a temperature increase from row 1 to 7 for all investigated cases, see Figure 4 a). Here, cases with larger amount of volume flow through the straight inlets shine out with lower differences. Otherwise, there are no major differences between all cases except 0/-100|, where, regard to the boundary effects of row 1 and 10, the best homogeneity with the smallest temperature difference (ΔT_{chest}) was observed. Due to these effects, row 1 and 10 were not considered for the calculation of ΔT_{chest} in Table 2. Here, values ≤2.0 K can be observed for all cases except 100/-0, 66/-33 and MIX.

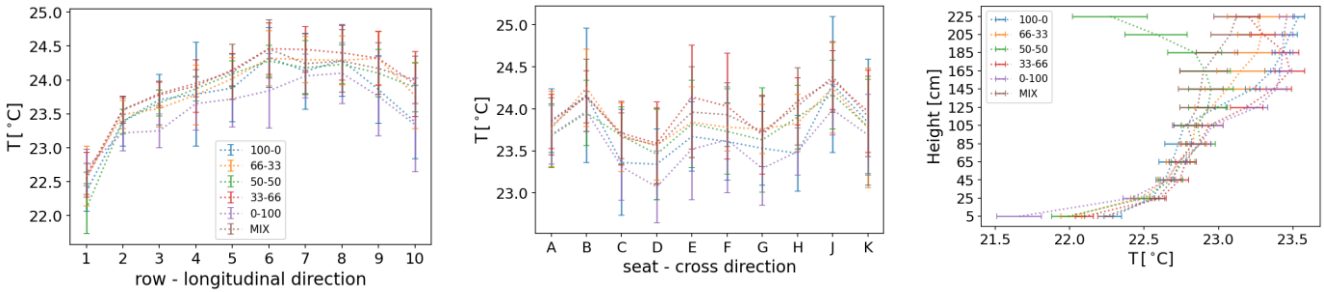

Figure 4: Fluid temperatures at chest position of the TMs averaged over a) seat rows and b) seat columns as well as c) fluid temperatures at aisle position for six different volume flow distributions.

The averaged values in cross-section, Figure 4 b), reveal lower temperatures for window (A, K) and aisle (C, D, G, H) seats as compared to the middle seats (B, E, F, J). Compared to the other configurations are case 100/-0| and 0/-100| the concepts with significant deviations in the mean. In addition, we found the highest standard deviations for the middle seats (J) and (B) for 100/-0|.

Table 2. Temperature evaluation parameters for different flow distributions

Case	$\Delta T_{h\text{-}a}^{max}$ [K]	$\Delta T_{h\text{-}a}^{mean}$ [K]	ΔT_{chest} [K]	$\langle U \rangle_{max}$ [m/s]	SF_6^{max} / Position [ppm]	PMV [-]	PPD [%]	HRE [-]
100/ - 0|	2.8	1.8	2.8	0.37	22 / 8G	-0.8	19	0.28
66/ - 33|	3.3	2.3	2.4	0.25	101 / 8J	-0.8	17	0.18
50/ - 50|	3.4	2.8	1.7	0.22	56 / 8J	-0.8	18	0.28
33/ - 66|	2.9	2.2	1.9	0.29	33 / 8J	-0.7	16	0.20
0/ - 100|	2.4	1.9	2.0	0.52	19 / 8J	-1.0	26	0.32
MIX	2.8	2.3	2.1	0.21	69 / 8J	-0.8	18	0.25

The temperature stratifications in the aisle region are depicted in Figure 4 c). Obviously, a higher proportion of slanted supply (100/-0| and 66/-33|) results in a higher temperature gradient for the complete cabin height. For the 50/-50| case, a temperature stratification up to a height of 85 cm, stationary temperatures in the middle part of the cabin and falling values in the ceiling area are found. A higher amount of straight volume flow reveals a temperature stratification up to 165 cm with approximate stationary values above this level. Due to the stratifications in the aisle section, MIX can be evaluated as best case with the lowest temperature increase from 45 cm to a height of 225 cm amounting to as little as 0.22 K/m.

Summarizing these findings, all temperature stratifications are within the requirements defined in the ASHRAE handbook (2001) as well as in the standard for train ventilation EN 13129 (2016).

3.2 Velocities. In addition to the local temperatures, the flow velocities in the passenger zone are an important criterion to evaluate passenger thermal comfort. Figure 5 depicts the mean fluid velocities averaged over 1800 s in row 6 at ankle, knee, chest and head level for all volume flow distributions.

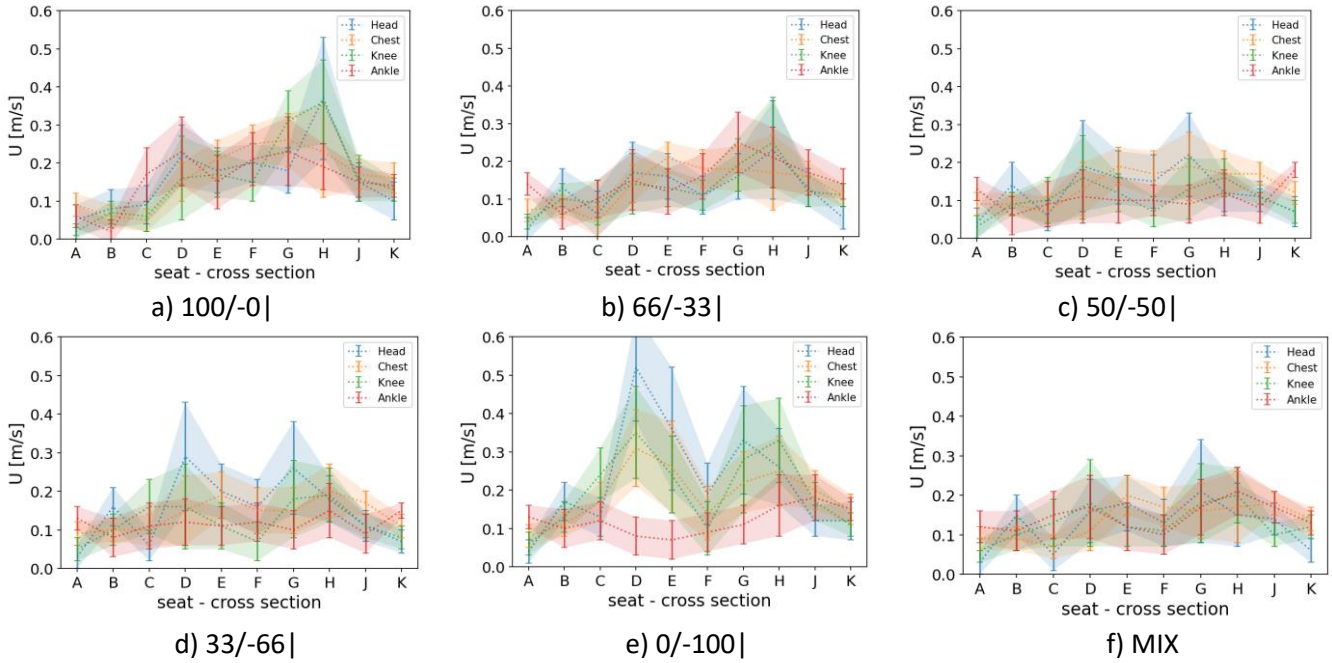

Figure 5: Comparison of fluid velocities in the vicinity of the TMs at four height positions for a) 100/-0|, b) 66/-33|, c) 50/-50|, d) 33/-66|, e) 0/-100| and f) MIX

Regarding the mean velocities, at all measurement positions for all cases except 100/-0| and 0/-100| satisfactory results can be observed starting from the maximum speed of 0.31 m/s as the upper limit in ASHRAE (2001). Thus, Table 2 shows velocities less than 1.6 m/s in green, larger than 3.1 m/s in red and intermediate values in yellow. Obviously, a supply of fresh air with only 18 air inlets (compared to 36 air inlets for all cases with volume flow rate split) results in high velocities at the central aisle seats (D and G) for 0/-100| as well as at aisle seat H for the 100/-0|case. Uncritical results can be found for 50/-50| as well as MIX with mean velocities of ≤ 0.22 m/s, see Table 2. Taking the standard deviations of 0.11 m/s into account, the maximal velocities lie slightly above 0.31 m/s. Except of the cases with higher amount of slanted air supply (100/-0| and 66/-33|), the highest velocities can be observed near the aisle in the middle row (seat 6D and 6G). Obviously, the major part of supply air was transported towards the center of the cabin for these cases. With 100/-0| and 66/33|, higher velocities in FDR and FRL can be observed.

3.3 Tracer-gas measurements. SF_6^{max} in Table 2 presents the maximum parts per million (ppm) concentrations of the SF_6 tracer gas averaged over eight time points of a stationary distribution of particles for all investigated cases. Here, green ($SF_6 \leq 30$) corresponds to a good rating, yellow ($30 < SF_6 \leq 90$) means an acceptable rating while red ($90 < SF_6$) indicates a comfort-critical rating. Except of 100/-0|, the highest ppm concentration was found for all cases at seat 8J, which is the middle seat in FDR next to the source. Further, the concentration rises with higher amount of slanted supply. The lowest values are found for the undivided inlet configurations (100/-0| and 0/-100|). However, all further measurement positions in the vicinity of the source - not visualized for the sake of brevity - reveal very low values for all cases.

3.4 Comfort relevant parameters. Using the comfort sense system, an evaluation of thermal comfort near the passenger on seat 6J was implemented using the PMV and PPD index, see Table 2. For PMV, an intermediate section of |1| to |2| with evaluation slightly warm / cold is marked in yellow after EN ISO 7730 (2005). Lower values, highlighted in green, reveal a neutral good evaluation, lager values in red show warm / cold ratings. Thereby, the PPD index is calculated based on the PMV value. The latter itself is an integral thermal comfort quantity and comprises air

temperature, radiation temperature, air velocity as well as humidity. For the corresponding PPD index, all values < 25% are markered in green, > 75% in red and intermediate values marked in yellow. All cases except of 0/-100 reveal acceptable comfort relevant parameter amounting to mean |PMV| < 1 and PPD < 25 %. It should be noted, that the different comfort evaluations might be compensated by adjusting the temperature of the supply air. The results of 0/-100| suggest a possible increase of T_{in} and, thus, energy saving by cooling down the supply temperature so far.

3.5 Heat-Removal-Efficiency (HRE). Finally, we calculate the heat removal efficiency (HRE = 0.5 * (T_{out} - T_{in}) * (T_{cab} - T_{in})$^{-1}$, see Table 2), which is a possible measure for the efficiency of the ventilation system. A perfect mixing in the cabin, i.e. $T_{cab} = T_{out}$, results in an HRE of 0.5. Here, green (0.5 ≤ HRE) corresponds to a good rating with T_{out} at least equally or higher as compared to T_{cab}. Yellow (0.3 < HRE < 0.5) means an acceptable rating while red (HRE < 0.3) indicates a comfort-critical rating. However, state-of-the-art MV concepts reach HRE values of about 0.4, see Bosbach (2013). Higher HRE values of novel ventilation systems represent a more efficient removal of the heat from the cabin by the air flow (Bosbach, 2013). In the present study, very low HRE values with a maximum of 0.32 for 0/-100|, were found for all cases. In previous numerical studies in a slightly different geometry, presented in Schmeling et al. (2020-1), we found similar HRE of 0.39 for this ventilation concept. As compared to state of the art MV with the aim for a perfect mixing of fresh and used air due to fast inflow velocities from both sides of the cabin, MJV shines out with lower flow velocities and thus, a lower blending of fresh and used air. In our study, the exhaust air ducts are mounted at the floor on both sides of the cabin, next to the Dado panels, i.e. the same exhaust locations as state-of-the-art mixing ventilation. To improve the HRE, lateral air exhausts above the windows just below the lateral overhead compartments and in the central overhead compartment above the middle seats will be considered in the further course of the project. The potential for this configuration was also confirmed in the previously cited numerical study by Schmeling et al. (2020-1) where a HRE of 0.55 was found for MJV with such a exhaust configuration.

A further possible evaluation of the efficiency of the ventilation system is the temperature difference between $T_{cab} - T_{in}$, being a measure for the requested supply air conditions of the HVAC system. For a stationary and comfortable value of T_{cab} = 23 °C, higher supply air temperatures mean lower cooling demand for the HVAC system. The best values are for 100/-0| and MIX found at supply air temperatures up to 19.6 °C, i. H. Tcab - Tin = 3.4K (Table 1). This value is almost twice as low as in modern mixing ventilation, where Tcab – Tin is ≈ 7 K, see Bosbach et al. (2013).

CONCLUSION

We present the first experimental results with micro-jet ventilation (MJV) in a full-scale twin aisle aircraft cabin mock-up. This ventilation concept is a generic version of the state-of-the-art ventilation concept often used in today's trains, and which was also previously investigated in numerical analysis for an aircraft cabin. To determine optimal comfort parameters for 100 thermal manikins, six different volume flow distributions between slanted and straight air supply were investigated under realistic boundary conditions for the normal flight phase "cruise". With defined boundary conditions, thermal comfort parameters based on fluid temperatures as well as velocities were evaluated using local probes. Further measurement techniques provided an overview about the thermal comfort, the propagation of containment as well as the efficiency of the different cases.

The first thing to note is, that there is unfortunately not one optimal case for all evaluation criteria. Differences depending on the volume flow distribution are found regarding the temperature between head and ankle as well as at chest level in row 2 to 9. Compared to the requirements defined in the standards, all cases are uncritical due to the thermal comfort. However, the mean fluid velocities in the vicinity of the TMs reveal values above the requested limit of 0.31 m/s for 0/-100| and 100/-0| where only half of the MJV inlets are used. Thus, a percentage distribution of supply air is necessary for ventilation of long-range aircraft cabins with MJV, or – in other words – large supply air areas are needed. The cases 50/-50| and MIX shine out with the lowest mean velocities.

The propagation of containment was detected at six points surrounding a source using SF_6 as tracer gas. At high flow velocities, for 100/-0| and 0/-100| to observe a reduced spread of the tracer gas. Acceptable values are found for 50/-50|, 33/-66| and MIX.

Regarding the comfort parameters PMV and PPD, all values are on the same basis with good evaluation except for the 0/-100|. Finally, a poor evaluation of the HRE values was found for all cases. To improve the HRE, lateral air exhausts above the windows just below the lateral overhead compartments and in the central overhead compartment above the central seat will be considered in the further course of the project. Overall, the volume flow distributions 50/-50| and MIX shine out with almost optimal comfort parameters.

Based on this extensive study of generic MJV, modifications of MJV inlets as well as lateral air exhausts will be investigated in future studies. In the pursuing course of the project, the cases 50/-50| and MIX will be compared with the reference case MV as well as other novel systems. Furthermore, the scenario "Hot Day on Ground", where the cooling-down process of the warm cabin after the boarding procedure with a fully occupied cabin as well as waiting for takeoff under hot ambient conditions, will be investigated.

ACKNOWLEDGMENTS

This project has received funding from the Clean Sky 2 Joint Undertaking under the European Union's Horizon 2020 research and innovation programme under grant agreement No 755596.

NOMENCLATURE

T_{out}	= Air Exhaust Temperature	T_{cab}	= Cabin air temperature
T_{in}	= Air Inlet Temperature	T_{amb}	= Ambient Temperature
TM	= Thermal Manikin	*HRE*	= Heat Removal Efficiency
FDR	= Flight Direction Right	*FDL*	= Flight Direction Left
RTD	= Resistance Temperature Detector	SF_6	= Sulphur Hexafluoride
PMV	= Predicted Mean Vote	*PPD*	= Predicted Percentage Dissatisfied
$\Delta T_{h\text{-}a}$	= Temperature difference of head and ankle	ΔT_{chest}	= Temperature difference of 80 chest RTDs

REFERENCES

ASHRAE. *ASHRAE Handbook of Fundamentals* Atlanta: ASHRAE, 2001
Bosbach et al., *CEAS Aeronautical Journal* 4, 301- 313, 2013
Bosbach et al., *ICAS2012*, Brisbane, Australia, September 23-28, 2012, ISBN 978-0-9565333-1-9
Dehne et al., *Roomventilation*, Espoo, Finland, June 2-5, 2018 #ID172
Dehne et al. *Roomvent*, Sao Paulo, Brazil, 2014
EN 13129:2016, *Railways Application; Air Conditioning for Main Line Rolling Stock*, 2016
EN ISO 7730, *European Commitee for Standardization*, Bruxelles, 2005.
IATA - International Air Transport Association, A global approach to reducing aviation emissions, 2009.
Lange et al., *AEC2020*, Bordeaux 25.-28. February 2020
Lange et al., *CEAS Aeronautic Journal*, to be submitted in April 2021
Martinez, *Aircraft Environmental Control*, P.U.o. Madrid, Madrid, Spain, 2014.
Schmeling et al., *AEC2020*, Bordeaux 25.-28. February 2020-1
Schmeling et al. *Building and Environment 182*, pp. 107 - 116., 2020-2
Schmidt, *Technical University of Denmark*, 2008
Yin et al., *Building Simulation*, 1030-1036, 2009
Zhang et al., *Building and Environment 42*, 1675-1684 (2007)